Triple acquisition mass spectrometry (TRAM) combining targeted and non-targeted metabolomics in a single run

Lisa Panzenboeck[a,b], Harald Schoeny[a], Bruno Stelzer[a], Elisabeth Foels[a,b,c], Marvin Glas[a], Marlene Pühringer[a,b], Dorian Hirschmann[c], Daniela Loetsch[c], Christian Dorfer[c], Evelyn Rampler[a,b] , Gunda Koellensperger[a,d]*

[a] Department of Analytical Chemistry, Faculty of Chemistry, University of Vienna, Waehringer Str. 38, 1090 Vienna, Austria

[b] Vienna Doctoral School in Chemistry (DoSChem), University of Vienna, Vienna, Austria

[c] Department of Neurosurgery, Medical University Vienna, Waehringer Guertel 18-20, 1090 Vienna, Austria

[d] Vienna Metabolomics Center (VIME), University of Vienna, Althanstr. 14, 1090 Vienna, Austria

ABSTRACT: We introduce TRAM, a triple acquisition strategy on high-speed, time-of-flight mass spectrometry for merging non-targeted and targeted metabolomics into one run. TRAM stands for "quasi-simultaneous" acquisition of (1) a full scan MS1, (2) top 30 data-dependent MS2 (DDA), and (3) targeted scheduled MS2 for multiple reaction monitoring (MRM) within measurement cycles of ~ 1 second. TRAM combines the selectivity and sensitivity of state-of-the-art targeted MRM-based methods with the full scope of non-targeted analysis enabled by high-resolution mass spectrometry. In this work, we deploy a workflow based on hydrophilic interaction chromatography (HILIC). For a broad panel of metabolites, we provide chromatographic retention times, and optimized conditions as a basis for targeted MRM experiments, listing accurate masses and sum formulas for fragment ions (including fully ^{13}C labelled analogs). Validation experiments showed that TRAM offered (1) linear working ranges and limits of quantification comparable to MRM-only methods, (2) enabled accurate quantification in SRM 1950 human plasma reference material, and (3) was equivalent to DDA-only approaches in non-targeted metabolomics. Metabolomics in human cerebrospinal fluid showcased the power of the strategy, emphasizing the need for high coverage/high throughput metabolomics in clinical studies. Acquiring up to 30 data-dependent spectra per MS cycle while still offering gold-standard absolute quantification, TRAM allows in-depth profiling and reduces required sample volume, time, cost, and environmental impact.

INTRODUCTION

The different facets of mass spectrometry-based metabolomics navigate the conflicting goals of analytical throughput and metabolome coverage. A comprehensive metabolomics experiment intrinsically requires multi-platform measurements.[1] As a result, different methods are combined into customized workflows, thereby reducing the number of analytical runs.[2]

High-resolution mass spectrometry allows for simultaneous non-targeted and targeted metabolomics. Nearly a decade ago, paradigms shifted, recognizing the power of high-resolution mass spectrometry for quantitative analysis. This paved the way for merging the two essential scopes of metabolomics, i.e., metabolite identification and quantification, into unified workflows.[2] Elaborate versions of merging targeted and non-targeted workflows integrate wide panels of external and internal standards and streamline MS1 and MS2 data acquisition (often resorting to separate injections). Non-targeted metabolomics requires high-resolution MS1 data for accurate mass determination and feature-based statistical analysis, together with high-resolution MS2 data for metabolite annotation (beyond sum formula annotation). Due to the low scan speed of state-of-the-art instruments (<50 Hz), data-dependent fragmentations are often performed on sample pools by replicate injections. Iterative exclusion lists - (automatically) generated between the injections - increase the depth of analysis.[3,4] The drawback of limiting metabolite annotations to pooled samples, where dilution effects hamper the discovery of rare and low abundant metabolites, has been extensively discussed.[5]

Most merged workflows use high-resolution MS1 data for targeted data analysis, which proved to be suitable for accurate absolute quantification in human plasma and other biological matrices.[6–8] However, there are examples establishing simultaneous non-targeted and targeted metabolomics. These workflows either utilize a combination of selected ion monitoring and MS1 scans on orbitrap systems[9], tribrid orbitrap systems (denoted as SQUAD)[10] or install dual MS platforms combined on-line to chromatography.[11]

Latest generation tandem high-resolution mass spectrometry unlocks the potential for unprecedented high throughput/high metabolome coverage strategies, offering MS2 acquisition rates > 100 Hz.[12] Multiple MS experiments can be merged within a single analytical run. In this work, we utilize this technological advancement and introduce a triple acquisition strategy (TRAM), increasing the sampling depth for both essential scopes of metabolomics, i.e., the identification and quantification of small molecules within one run. More specifically, we combine MS1, data-dependent acquisition (DDA), and scheduled targeted MS2, the latter enhancing sensitivity by allowing multiple reaction monitoring (MRM)-like evaluation on a recently introduced quadrupole-time-of-flight system. Compared to classical QTOF instruments, Zeno trapping[13] increases the ion efficiency to more than 90% by trapping ions after

fragmentation in a linear ion trap. By ramping AC voltages, ions are scanned out of the Zeno trap in a mass-dependent manner in order to tackle common mass intensity biases[12], which results in a four to 20-fold increase in sensitivity.[14] The utility of the Zeno function for biological applications has recently been demonstrated by Huang *et al.* in a mass isotopologue distribution study on stem cell-derived neurons.[15]

Exploiting the scan speed of up to 133 Hz[12], data-dependent MS2 acquisition can be tailored to ensure high numbers of MS2 spectra upon each sample injection. Additionally, scheduled MS2 was designed and optimized for MRM-like data evaluation. The hereby generated information-rich high-resolution MS2 spectra can be evaluated for targeted quantification and library matching.

Overall, the TRAM methodology was optimized to ensure a minimum of 8 data points per chromatographic peak in both the MS1 and MRM modality and to maximize the number of MS2 spectra per sample. Generating non-targeted and targeted information within a single injection reduces required sample volumes, which is especially important for clinical settings with low amounts of precious patient samples. By avoiding the need for (iterative) injections of sample pools or additional instrumentation, higher sample throughput can be achieved, thus lowering batch analysis times, solvent consumption, costs, and environmental impact. The novel workflow is compared to standalone MRM and DDA methods for quantification and non-targeted screening, respectively. Along with the novel analytical workflow, we provide a comprehensive list of transitions, declustering potentials (DPs), and collision energies (CEs) for 91 metabolites in positive ion mode on the ZenoTOF 7600. As a proof of concept, we analyzed the human plasma certified reference material SRM 1950 and cerebrospinal fluid (CSF) samples from meningioma patients with the optimized TRAM workflow. Due to the limited availability of CSF samples from patients, it is the ideal matrix to test the potential of merged targeted and non-targeted metabolomics in a single analytical run.

EXPERIMENTAL SECTION

Sample preparation. Cerebrospinal fluid (CSF) of meningioma patients was centrifuged and stored at - 80 °C after collection during surgery. Metabolites were extracted from CSF samples and human plasma standard reference material (SRM 1950, NIST, USA) by protein precipitation using 80% cold methanol after the addition of a fully ^{13}C labelled yeast extract as internal standard.[6] Derivatization of primary thiols was achieved with the help of N-ethylmaleimide.[16] Solvents were evaporated to dryness by vacuum centrifugation, and dried samples were stored at - 80 °C and reconstituted in 3:7 H_2O:IPA[17] prior to analysis. Based on a 50 µM equimolar mixture of ~ 160 metabolite standards (**Supporting Information (Table SA1)**), a calibration curve with a ratio of 1:8 ISTD to total volume was prepared in 3:7 H_2O:IPA. The calibration curve covered 16 concentration levels from 0.01 nM to 25 µM. A detailed description can be found in the **Supporting Information**.

LC-MS methods. A HILICON iHILIC-(P) Classic (100 x 2.1 mm, 5 µm, 200 Å) column coupled to a HILICON iHILIC-(P) Classic (20 x 2.1 mm, 5 µm, 200 Å) pre-column (both Dichrom, Haltern am See, Germany) and a Viper Inline Filter (Thermo Fisher Scientific) was used for metabolite separation on an Infinity 1290 LC System (Agilent). The column was mounted directly onto the source of the ZenoTOF 7600 mass spectrometer using a Micro Column Heater (AB SCIEX) and heated to 40 °C. The temperature of the autosampler was set to 10 °C, and an injection volume of 5 µl was selected. A description of the HILIC gradient adapted from Kim *et al.*[18] and El Abiead *et al.*[19] is provided in the **Supplementary Information**.

The OptiFlow Turbo V source of the ZenoTOF 7600 equipped with the 50-200 µl needle insert was used (OptiFlow 50-200µL Micro/MicroCal). Ion source gas 1 was set to 50 psi, and Ion source gas 2 to 60 psi. A Curtain gas flow of 35 and a CAD gas flow of 7 were used. The source temperature was 600 °C. Data was acquired in positive ion mode with a spray voltage of 4000 V. For TOFMS scans, a DP of 40 and CE of 10 were applied without spread. Samples were measured using MRM, DDA, and the novel combined TRAM MS method. Autocalibration was performed after two injections, and quick checks of the system were passed before and after the sequence was acquired. Zeno pulsing was activated for all precursor ions with an intensity lower than 20,000 cps. Q1 was operated at unit resolution. The mass range for TOFMS measurements was 65 Da to 900 Da for TRAM and DDA and 65 Da to 950 Da for MRM.

For DDA measurements, the maximum number of candidate ions was set to 40 with an intensity threshold of 100. The small molecule workflow was selected. Dynamic background subtraction was performed, and former candidate ions were excluded for 8 seconds after two occurrences. Since samples contained ^{13}C labelled yeast as internal standard, an exclusion list was generated using an ISTD solvent blank. The accumulation time for TOFMS scans was set to 0.4 s. For TOF MS2 scans, a start mass of 20 Da and a stop mass of 950 Da were selected, and the accumulation time was 0.005 s. The DP was set to 40 V and the CE to 25 V (both without spread). For the TRAM method, the maximum number of candidate ions was set to 30 and the TOFMS accumulation time to 0.1 s while preserving all other DDA parameters. To avoid redundant MS1 scans, the additional TOFMS scan of the MRM branch was deleted. For MRM and TRAM methods, a mass table containing precursor masses of interest, TOF start and stop masses, as well as corresponding retention times (RTs), RT tolerances, accumulation times, and optimized DPs and CEs (without spread) was sorted by precursor ion to improve sensitivity. **Supporting Information (Table SA2)** provides an overview of MRM transitions. A description of MRM parameter optimization is provided in the Experimental section of the **Supporting Information**. Accumulation times were adapted individually for TRAM and MRM methods to guarantee at least 8 points per peak, and scan scheduling was applied. ^{13}C labelled compounds had the same accumulation times, DPs, CEs, and RT settings as their non-labelled equivalents. TOFMS accumulation times were set to 0.1 s.

Data analysis. For quantitative sample analysis, peaks were integrated in SCIEX OS Version 3.3.1.43 using MQ4 for integration and the relative noise algorithm. The minimum peak width was set to 8 points, an XIC width of 0.02 Da was chosen, and the minimum height was 100. A S/N integration threshold of 3 was selected, and the Gaussian smooth width was set to 3.0 points. All other parameters were adapted individually for the respective compounds. MS1 signals were analyzed by processing files generated with all three methods within a single result file. MS2 data analysis was performed separately for MRM and TRAM files using the same integration parameters. A representative component list, providing MS1 as well as fragment masses of interest and corresponding processing

parameters, can be found in the **Supporting Information (Table SA3)**. To allow absolute quantification of metabolites, external calibration combined with internal standardization was applied by calculating the ratios between the ^{12}C peak areas and corresponding ^{13}C peaks. For comparison of working ranges across the three MS methods (MRM, DDA, TRAM), only compounds for which a corresponding ^{13}C signal was detected were used. To assess lower- and upper limits of quantification (LLOQs and ULOQs) of the individual MS methods, the respective calibration samples were set as standards, and metabolite concentrations were assigned before performing automatic outlier removal in SCIEX OS Analytics. Criteria for automatic outlier removal and working range assessment are described in more detail in the **Supporting Information**. Surrogate ISTD selection was based on similarities in ^{12}C peak areas in a 1 µM standard. Micromolar metabolite concentrations in SRM and CSF were calculated by selecting the six closest calibration points with regard to peak area ratios.

The number of triggered MS2 spectra was determined with the IDA Explorer function of the SCIEX OS Explorer by counting the number of MS2 spectra without applying the merging function. Non-targeted screening was also performed in SCIEX OS Version 3.3.1.43, applying the MQ4 and relative noise algorithms. All parameters relevant to non-targeted data processing are listed in the **Supporting Information.** For feature-based molecular networking, .wiff2 files from DDA and TRAM measurements of technical (n=3) replicates of CSF samples were imported to MS-DIAL (5.3.240328.alpha)[20], and the respective acquisition method was set as Class ID and DDA was chosen as Acquisition parameter. After adaption, alignment results, and .mgf files were used for feature-based molecular networking in GNPS2.[21,22] An extensive description of all MS-DIAL and GNPS data processing steps can be found in the **Supporting Information.** Statistical analysis of CSF samples was performed in MetaboAnalyst 6.0.[23,24] TRAM MS2 area ratios of 27 metabolites to (surrogate) ISTDs, exported from SCIEX OS, were used as input. Samples were divided into two groups according to their grade of malignancy: The first group included samples classified as WHO grade 1, and the second group featured samples ranked as WHO grade 1-2 and 2.[25] More detailed information can be found in the **Supporting Information**.

RESULTS & DISCUSSION

A HILIC-based metabolomics assay. Hydrophilic interaction chromatography is essential to customized workflows in non-targeted metabolomics, being the method of choice for the separation of the polar central metabolome. The combination with high-resolution mass spectrometry is straightforward. Metabolite isomers can be separated without derivatization or ion pairing reagents. However, there is not a single method for separating all isomers (as the case in ion pairing chromatography). **Figure 1A** illustrates the HILIC separation established in this study in a violin plot.[18,19] At pH > 9, most central metabolites are anionic, a key factor determining the HILIC retention mechanism and the ionization efficiency. The relatively short separation time of 12 min (and extensive re-equilibration of 15 min) allows for the separation of the critical isomers Uridine-Pseudouridine and Betaine-Valine **(Figure 1B)**. Other isomers such as Leucine-Isoleucine, Alanine-Sarcosine, Guanosine-Isoguanosine, and 3'-AMP-5'-AMP show only poor chromatographic separation, while hexoses and pentoses are not separated at all.

As a starting point and future research resource, ZenoTOF-MS specific declustering potentials and collision energies were optimized for 91 metabolites at alkaline pH. Currently, the wide target panel covers the metabolite classes of 1) (5'->5')-dinucleotides, 2) 5'-deoxyribonucleosides, 3) Biotin and derivatives, 4) Carboxylic acids and derivatives, 5) Diazines, 6) Fatty Acyls, 7) Glycerophospholipids, 8) Imidazolpyrimidines, 9) Indoles and derivatives, 10) Nucleoside and nucleotide analogues, 11) Organic sulfonic acids and derivatives, 12) Organonitrogen compounds, 13) Organooxygen compounds, 14) Phenols, 15) Purine nucleosides, 16) Purine nucleotides, 17) Pyridines and derivatives, 18) Pyrimidine nucleosides, 19) Pyrimidine nucleotides, and 20) Ribonucleoside 3'-phosphates as shown in **Figure 1C**.[26] For all compounds, a list of potential quantifier fragments (including the fully labelled ^{13}C pendant), optimized collision energies, and ranges of declustering potentials for the ZenoTOF 7600 is reported (**Supporting Information Tables SA4 & SA5**).

High-resolution triple acquisition mode (TRAM) for combined targeted and non-targeted metabolomics. High-resolution TRAM combines simultaneous full scan mode (i.e., MS1), data-dependent MS2 acquisition (top 30 DDA), and scheduled targeted MS2 acquisition. The latter modality allows optimum ion transfer- and fragmentation conditions for each target, unifying the selectivity and sensitivity of MRM with the full scope of high-resolution MS2 spectra. For simplicity, we will use the term MRM from now on. Zeno trapping was activated on the MS2 level for both DDA and MRM acquisition modes to boost sensitivities.

TRAM merges multiple MS experiments and data evaluation strategies into one analytical run. Targeted metabolomics data can be obtained either at the MS2 level (MRM) or the MS1 level. Non-targeted metabolomics screening relies on high-resolution MS1 for (1) feature-based statistical analysis (relative quantification task) and (2) deriving sum formulas from accurate mass. Data-dependent MS2 scans are the gold standard for high-confidence structure annotation. State-of-the-art methods achieve in-depth DDA-based fragmentation by iterative sampling, requiring multiple injections. This type of analysis resorts to pooled samples to reduce the number of analytical runs. Data-independent acquisition strategies increase the throughput for high coverage analysis, accepting a de-facto higher false discovery rate.[27] The high speed of the ZenoTOF technology, enabling up to 133 Hz, allows for the adoption of DDA for in-depth metabolic profiling, reducing the risk of chimeric spectra compared to data-independent acquisition. **Figure 2** depicts the duty cycle of the proposed TRAM approach. Allowing cycle times of ~ 1 second, TRAM boosts the number of triggered tandem MS measurements per sample. The exact timing of each cycle depends on the number of scheduled MRM spectra at a given retention time and varies over the chromatographic run. To maximize the signal-to-noise ratio, the optimized accumulation times of MRM spectra exceed those of DDA spectra. This study limited the cycle time to a 1-second range, as otherwise, the number of data points per chromatographic peak is reduced, limiting the accuracy of peak integration. The chromatographic region with the highest number of scheduled MRM scans is the basis for calculating the maximal number of DDA scans possible and accumulation times. Given this condition, each MS cycle contains one MS1 spectrum, up to 30 DDA tandem MS spectra (accumulation time of 5 ms), and up to 24 MRM transitions (minimum accumulation times of 10 ms).

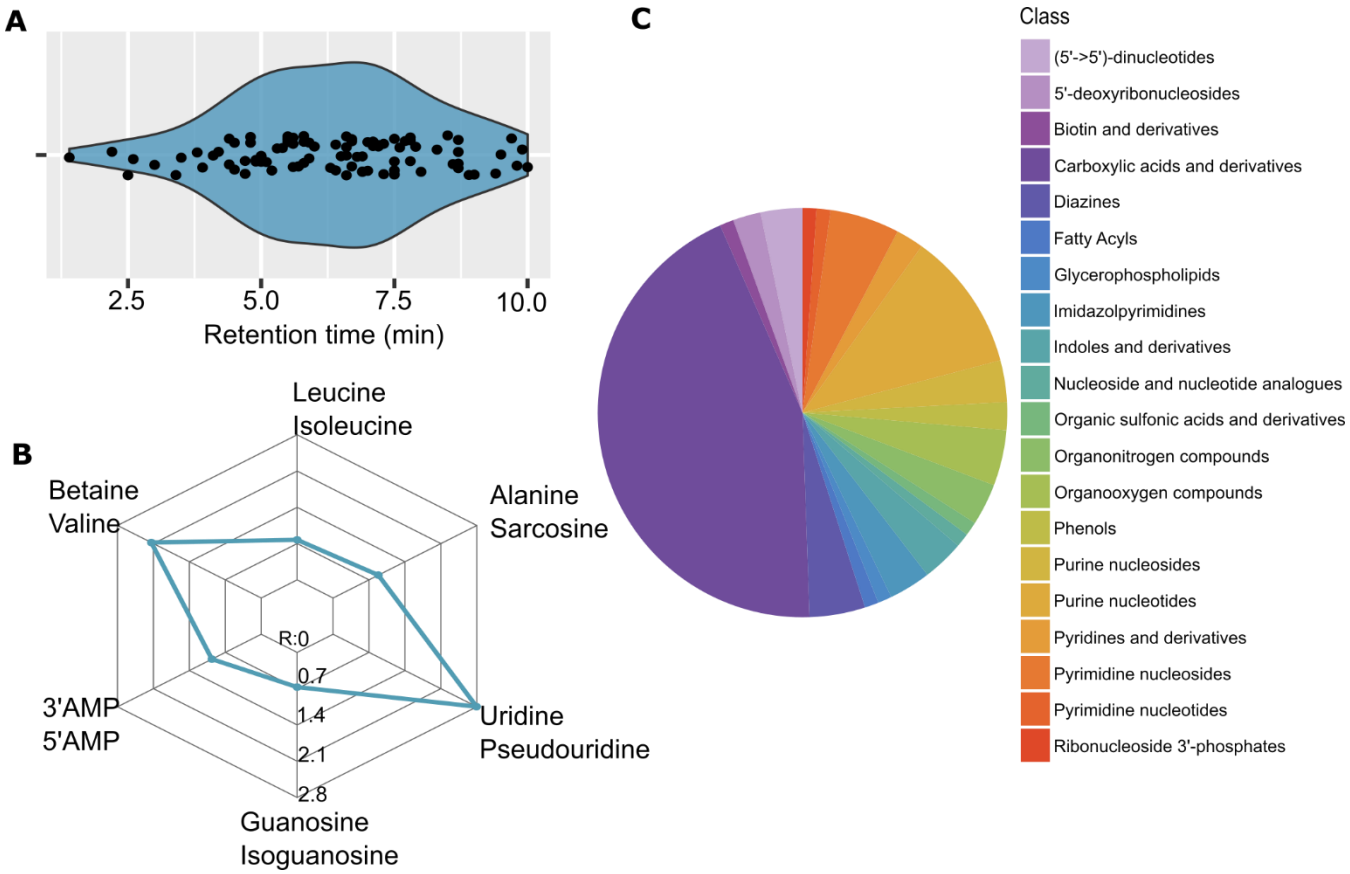

Figure 1: When alkaline HILIC separation is applied, most metabolites under investigation elute between 2.5 and 10 minutes (A). Isomer pairs like Uridine-Pseudouridine and Betaine-Valine (R>1.5) can be separated, while baseline separation cannot be achieved for other isomer pairs like Leucine-Isoleucine, Alanine-Sarcosine, Uridine-Pseudouridine, Guanosine-Isoguanosine, and 3'AMP-5'AMP (B). The proposed HILIC-MS workflow allows the analysis of 20 metabolite classes (C).

Working range and limit of quantification for targeted analysis – TRAM versus MRM- and DDA-only. Targeted analysis by TRAM was benchmarked versus DDA-only and MRM-only, the latter being the gold standard for quantitative analysis. We established key analytical figures of merit for targeted analysis using a dilution series of metabolite standards spiked with uniformly ^{13}C labelled yeast-derived internal standards. A concentration range over more than 6 orders of magnitude (10 pM to 25 µM) was used to determine the linear dynamic working range. Stringent criteria for outlier removal were applied to assess LLOQs and ULOQs (see **Experimental Section** & **Supporting Information**). For TRAM and MRM-only, MS1 and MRM MS2 levels could be combined to determine LLOQs and ULOQs. For DDA-only calibration functions were based solely on the MS1 level.

Figure 3A plots the obtained working ranges comparing species-specific isotope dilution for 19 metabolites by TRAM versus MRM-only and DDA-only. The target metabolites were selected based on the fact that these compounds were abundant in the ^{13}C labelled yeast and thus amenable to internal standardization for all investigated MS strategies. Both MRM and TRAM were equivalently fit for the quantification purpose, showing working ranges of 3-4 orders of magnitude and comparable average LLOQ values in the low nM range. Both strategies clearly outperformed the DDA approach in all investigated figures of merit. **Supporting Information Table SB1** summarizes the obtained calibration slopes, intercepts, correlation coefficients, LLOQs, and ULOQs. A mass accuracy filter of 5 ppm was applied for MS1-level data. It has to be stated that the determined LLOQ values are procedural LLOQ values, determined by procedural blanks, and intrinsically higher than sole instrumental LLOQs (especially considering the yeast-derived internal standard). To compare the sensitivity of the acquisition methods, we determined the fraction of ^{12}C target panel metabolites for which the signal-to-noise ratio exceeded a value of 3. As shown in **Figure 3B,** TRAM shows excellent sensitivity in MRM-MS2 acquisition mode, boosting signal-to-noise ratios even at very low concentrations of 10 pM. A comparison of fragment mass errors, which are equally low for MRM-only and TRAM acquisition, is presented in **Supporting Information Figure S1**.

Finally, targeted TRAM was benchmarked for surrogate internal standardization. The selected ^{13}C surrogate internal standards fulfilled the criteria of (1) comparable ionization efficiency as approximated by peak areas of unlabelled metabolites in a 1 µM standard and (2) being abundantly present in the uniformly ^{13}C labelled yeast extract. Working ranges were assessed as described previously using the SCIEX OS automatic outlier removal algorithm. Based on this approach, LLOQs as low as 0.1 nM were found, and ULOQs ranged up to 25 µM. An extensive overview of calibration ranges for TRAM-based quantification using surrogate ISTDs is provided in **Supporting Information Table SB2**.

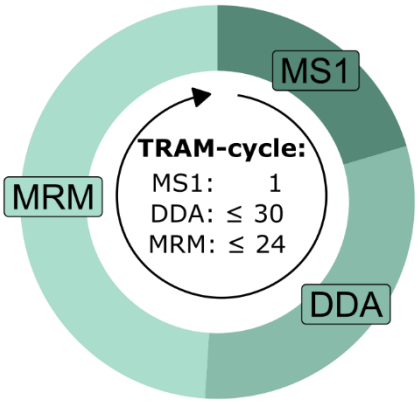

Figure 2: A theoretical MS cycle of the novel TRAM method is represented when one MS1 scan is followed by 30 DDA triggers and 24 scheduled MRM transitions. Please note that actual cycle times might vary due to instrument switching times and need to be determined during method optimization.

Summarizing, the combined TRAM approach allows the quantification of many metabolites across a wider working range than the stand-alone DDA method, with the additional benefit of generating up to 30 DDA MS2 spectra per MS-cycle compared to stand-alone MRM.

Accuracy of quantification. The accuracy of quantification was assessed for 14 metabolites with certified concentrations using the reference material for human plasma SRM 1950, issued by NIST.[28] Additionally, six compounds with available indicative concentration values published by Thompson et al.[7] (Propionyl-L-Carnitine, Aspartic Acid, Glutamine, Glutamate, Kynurenine, and Taurine) were included. For all compounds, species-specific isotope dilution by ^{13}C labelled yeast was enabled, with the exception of Glycine, nemylated Cysteine, Propionyl-L-Carnitine, Kynurenine, and Taurine, resorting to surrogate internal standards on both MS1 and MS2 level, and Isoleucine and Methionine on MS1 level. As reported elsewhere[29], the quantitative exercise was based on calibrations fitted by selecting, out of the extensive calibration data set, 6 calibration points closest in area ratio to the mean SRM area ratio of triplicate measurements. As a result, the calibration covered tailored concentration ranges for the respective targeted metabolite (maximum 2.5 orders of magnitude). This strategy and the fact that certified and indicative concentration values were in the µM range enabled cross-validation of MS1- and MS2-level quantification in TRAM. Only calibrations with R values exceeding 0.9 were accepted. A comprehensive overview of the calibration curves for SRM quantification is provided in **Supporting Information Table SB3**.

85% of the investigated metabolites were in good agreement with target values (agreement within 20%; see **Supporting Information Figure S2**). 70% of the metabolites showed even higher agreement < 10%. The indicative value of Taurine could not be recapitulated regardless of whether TRAM was evaluated based on MS1 or MS2 level. Establishing calibrations with tailored concentration ranges, most compounds could be quantified with a recovery of <20% on both MS1 and MS2 level. Glycine, Isoleucine, Serine, Valine, and Kynurenine required the selectivity of MS2 level measurement for accurate quantification.

Evaluating non-targeted metabolomics enabled by TRAM. Data-dependent MS2 spectra are the gold standard for high-confidence compound annotation, library matching, and feature-based molecular networking in non-targeted applications. While common metabolomics workflows require iterative exclusion list generation based on sample pools, the combined TRAM workflow allows the generation of sample-specific data-dependent spectra along with sensitive absolute quantification. Non-targeted screening can thus be performed on an individual basis, generating data-dependent scans of features

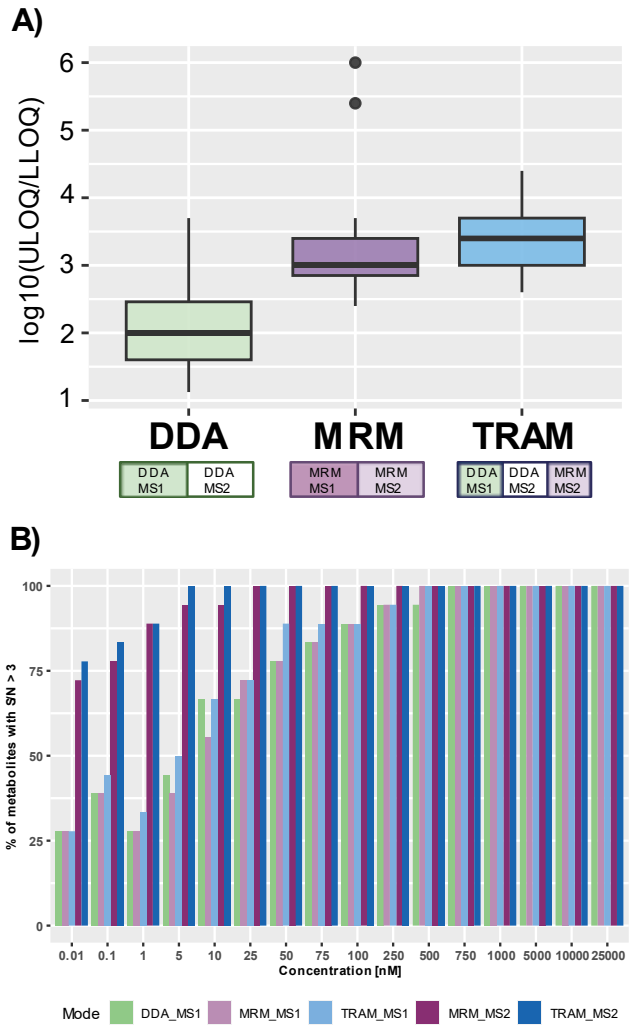

Figure 3: A) Working ranges of stand-alone DDA (green) and MRM (violet) methods compared to the combined TRAM (blue) workflow. Colored method blocks highlight the acquisition strategies used for the working range assessment. TRAM and MRM-based quantification yield similar working ranges, outperforming DDA. B) Percentage of metabolites listed in **Supporting Information Table SB1** exceeding the signal-to-noise threshold of 3 with respect to the MS-acquisition mode. For MS2-based acquisition strategies, more than 70% of the compounds exceed the defined threshold already at the lowest concentration of 0.01 nM. The slight differences between MRM MS2 and TRAM MS2 for low concentrations originate from Glutamine, which was found to have a S/N bigger than 3 for TRAM but not for MRM for low concentrations.

that would usually be diluted in sample pools or require iterative sample injections - which are often not possible for low sample volumes. Limiting the cycle time to a 1-second range, TRAM enables up to 30 DDA scans for each cycle. TRAM was scrutinized and compared to DDA-only (top 40) upon analysis of SRM 1950 (n=3 injections). Average numbers of data-dependent MS2 triggers were calculated per sample and acquisition method and varied between 5004 (SRM – DDA) and 5555 (SRM – TRAM) with RSDs below 2.4%. The number of MS2 spectra triggered with TRAM was within 10% of the DDA-only triggers. When assessing the number of MS2 triggers, one has to bear in mind that it depends on the sample, triggering thresholds, and the maximum number of data-dependent scans allowed.

Preprocessing steps determine the feature matrix[30] and need to be optimized for each method. We performed non-targeted data processing for DDA-only and TRAM to compare the number of features, MS2 spectra, potential library matches, and features for which sum formulas could be predicted. The same settings were used for both methods within a retention time window of 0.9 to 14.1 minutes (see **Experimental Section** and **Supporting Information**). Non-targeted analysis of SRM 1950 yielded more than 6750 features for DDA runs and about 4460 for TRAM. This resulted in a similar decrease in formula finder results (DDA: 4890, TRAM: 3338). In spite of this reduction in features (-33%), the number of MS2 spectra was only reduced by 17%, and the number of library hits with scores bigger than 70% was reduced by 11%. For both MS methods, 5 to 6% of MS2 spectra had a library hit with a score bigger than 70%, which is similar to the ratio of library hits to MS2 spectra reported by Proos and Baker in their application note[12] on non-targeted metabolomics on the ZenoTOF 7600.

Showcasing the power of TRAM in clinical studies. The power of TRAM was assessed in clinical cerebrospinal fluid samples for the two essential analytical tasks of metabolomics, i.e., targeted absolute quantification and non-targeted analysis. The cerebrospinal fluid was obtained in the frame of an ongoing clinical study on meningioma tumors, exploring, besides other aspects, the potential of metabolomics to predict meningioma grading. While several promising metabolomics/lipidomics reports on tumor tissue biopsies exist, proof of principle studies in cerebrospinal fluid are lacking. Amino acids and small organic acids were discovered to be among the potential signature metabolites[31–33] in tumor tissue. The meningioma grade could be distinguished based on metabolic pathways such as glycine/serine metabolism, choline/tryptophan, purine and pyrimidine metabolism.[31] The same study revealed an additional set of changing metabolites by unsupervised statistical analysis. Taurine, creatine, serine, choline, thiamine, phenylalanine, biotin, glutamine, and arginine were proposed as signature metabolites by hierarchical clustering.[31]

The MRM targets were selected accordingly, focusing on amino acids and organic acids found relevant in meningioma research. Finally, the target list also included Phosphocholine, Glycerophosphocholine, and N-Acetyl-aspartate, with the aim of distinguishing meningioma from glial and oligodendroglial-like brain tumors, as IDH mutations are currently debated in meningioma samples.[34]

Absolute quantification of metabolites in CSF. Due to the lack of certified reference materials, in clinical metabolomics, quality controls are produced in-house from pooled samples as established by community guidelines.[35] In this study, a pooled quality control sample of 16 cerebrospinal fluid samples (5 control, 11 meningioma patients) served to assess benchmark absolute quantitative values. Metabolite concentrations in the quality control pool varied from low nanomolar (30 nM) to high micromolar (>ULOQ) concentrations. A comprehensive overview of the included target panel and corresponding concentrations obtained in the CSF-QC sample is given in **Supporting Information Table SB4**. **Figure 4** illustrates that quantified concentrations in the CSF-QC sample pool represented by violet dots are within the same orders of magnitude as those listed in the HMDB[26] for adults (green boxplots). The high agreement between experimental and literature values for CSF metabolites demonstrates that TRAM is fit for metabolite quantification in clinical matrices.

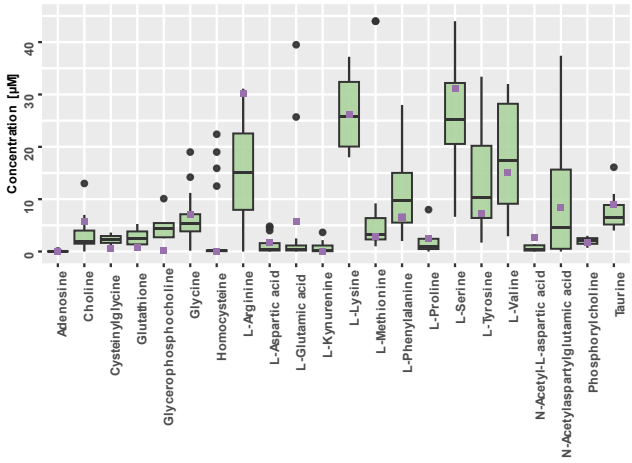

Figure 4: Concentrations of metabolites in pooled CSF-QC samples (cancerous and control) -violet – compared to concentrations extracted from HMDB[26] for adults. The plot was limited to concentration values below 45 µM. Data for Glutamine is not shown but was similar to reported concentrations (CSF-QC: 455 µM, Reference: 152-1157 µM).

Non-targeted analysis in clinical CSF samples. Feature-based molecular networking (FBMN) visualizes and analyzes these highly complex data sets, incorporating MS1 and MS2 information. To showcase the versatility of the novel TRAM acquisition strategy for clinical metabolomics, we performed FBMN in GNPS 2 after preprocessing DDA and TRAM data of CSF replicates in MS-DIAL. A representative subnetwork is depicted in **Figure 5A,** with feature intensities for DDA represented in orange and violet for TRAM. Details on processing parameters can be found in the **Supporting Information**. As can be seen, most nodes have a 50:50 distribution of DDA- and TRAM, indicating equal intensities for the features irrespective of the acquisition strategy. The network consisted of 2372 nodes and 3065 edges. 9% of the nodes showed a variation of more than 50% in intensities across MS methods, and below 1% of the clusters were only present when measured with either DDA or TRAM, demonstrating the versatility of TRAM for complex non-targeted workflows. Replicate injections of pooled CSF samples, containing no ISTD, were measured by DDA-only and TRAM. TOFMS accumulation times were set to 0.1 seconds for stand-alone DDA measurements. None of the methods contained an exclusion list. Most of the time, the 30 triggers set for TRAM are only fully exploited in very dense chromatogram regions. Comparing the top 40 DDA method to TRAM,

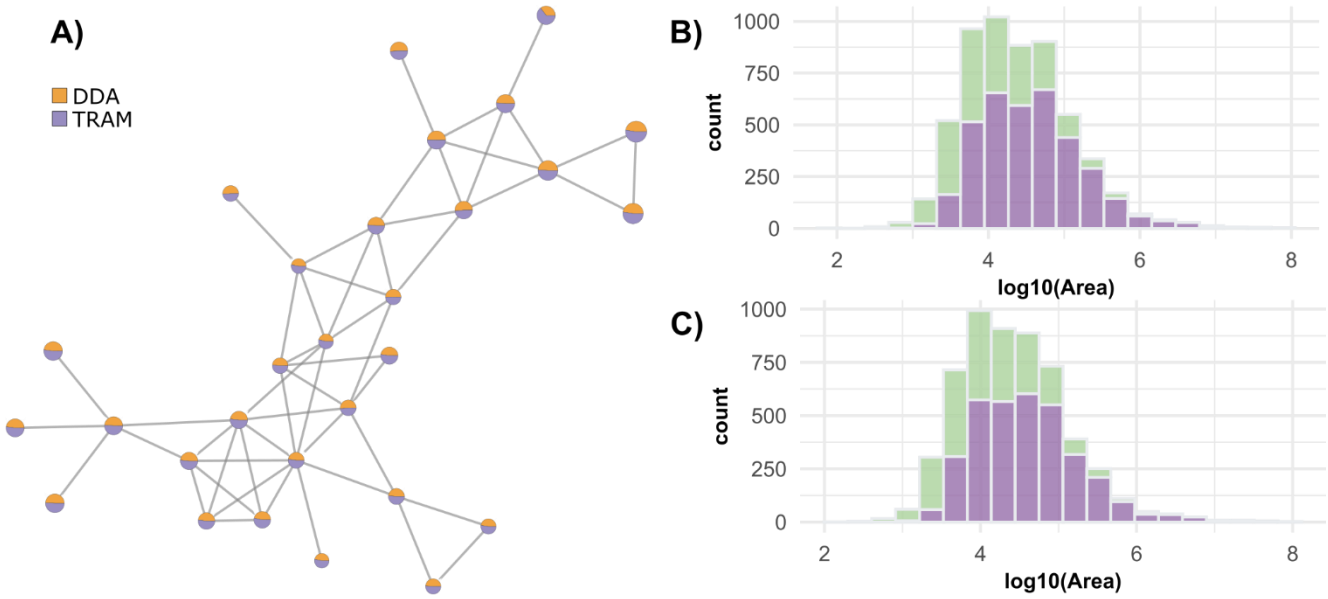

Figure 5: A) By combining MS1 and data-dependent MS2 information, feature-based molecular networks can be created from CSF metabolomics data. Most features can be found with DDA (orange) and TRAM (violet). Features found with DDA (B) and TRAM (C) measurements of a pooled CSF sample without (green) and with (violet) MS2 spectra. The total number of features, MS2 spectra, MS2 spectra with library hits (>scores 70%), and formula finder results was reduced by less than 10% in TRAM compared to DDA.

changes in numbers of detected features, MS2 spectra, library hits, and found formulas were below 10%, as shown previously for SRM 1950. An overview of the number of features with (violet) and without (green) MS2 spectra is presented in **Figure 5** for DDA (**B**) and TRAM (**C**) data of a representative injection of a CSF-Pool. While accumulation time can be increased for stand-alone DDA while still offering low cycle times and high numbers of DDA triggers, accumulation times need to be set as low as possible for TRAM methods. Despite the decrease in features, TRAM offers the possibility to generate a high number of data-dependent MS2 scans with sufficiently high spectral quality to be matched against library spectra (**Supporting Information Figure S3-S8**).

Metabolomics of cerebrospinal fluid in meningioma patients. As previously mentioned, the cerebrospinal fluid samples were collected in the frame of an ongoing clinical study aiming to distinguish between different WHO grades of meningioma. While the small number of samples (n=15) does not allow comprehensive statistical analysis, we still wanted to investigate whether metabolic patterns can be seen. Promising preliminary data suggests that meningioma grades can be partially differentiated based on MRM-MS2 $^{12}C/^{13}C$ area ratios acquired with TRAM (**Supporting Information Figure S9**). These preliminary findings indicate that LC-MS-based metabolomics can not only be applied to tumor tissue samples, as already described in literature[31–33], but also to CSF collected from patients. Future studies with larger cohorts and different brain tumor subtypes will further explore this potential and could find metabolite patterns for which intraoperative diagnostics by sensors can be envisaged combined with methylation profiles.[36] For samples like CSF, where sample volumes are limited, workflows like TRAM are required to offer the possibility of acquiring targeted and non-targeted data from a single injection.

CONCLUSION

Our study introduces TRAM as a triple acquisition strategy utilizing high-speed time-of-flight mass spectrometry, effectively combining non-targeted and targeted metabolomics in a single analytical run. The integration of HILIC with TRAM for polar metabolite analysis demonstrates comparable linear working ranges and limits of quantification to the gold standard of MRM only while enabling comprehensive metabolite profiling. We validated the TRAM approach using the human plasma certified reference material SRM 1950 and analyzed clinical CSF samples. TRAM proves highly suitable for analyzing samples with limited amounts, offering quasi-simultaneous quantitative and qualitative metabolite information while reducing cost, analysis times, and solvent consumption. For a wide target panel of polar metabolites separated by HILIC, retention times and optimized conditions for MRM experiments are reported. We also recognize significant potential in triple acquisition methods with other instrumental setups, including different high-resolution mass analyzers such as TOFs or Orbitraps, especially in cases of limited sample materials. In general, CSF is a promising, minimally invasive sample matrix offering information on relevant metabolites in meningioma and other diseases.

ASSOCIATED CONTENT

Supporting Information

The Supporting Information is available free of charge on the ACS Publications website.

Supporting Information including details on the experimental workflow as well as supplementary figures on targeted and non-targeted data analysis and statistical analysis of CSF metabolites in meningioma patients. (Supporting_Information.pdf)

SuportingInformation_TableA including an overview of metabolite standards, acquisition and processing parameters for TRAM data, a list of ^{12}C & ^{13}C fragments with optimized collision energies, and declustering potentials. (.xlsx)

SuportingInformation_TableB including working ranges for MRM-only, DDA-only, and TRAM data, as well as an overview of calibration points and mass errors for SRM 1950 quantification and a list of metabolites used for CSF quantification and statistical analysis. (.xlsx)

AUTHOR INFORMATION

Corresponding Author

* Gunda Koellensperger - Department of Analytical Chemistry, Faculty of Chemistry, University of Vienna, Waehringer Str. 38, 1090 Vienna, Austria
https://orcid.org/0000-0002-1460-4919;
Email: gunda.koellensperger@univie.ac.at

Author Contributions

Conceptualization and coordination of the project were performed by L.P. and G.K. The MRM parameters were optimized by L.P. and M.G. L.P., and M.P. developed the LC-MS method. CSF sample collection was coordinated by D.H., D.L., and C.D. and collected by D.H. Samples were prepared for LC-MS analysis by H.S., B.S., E.F., and L.P. L.P. and H.S. were responsible for data acquisition and evaluation. Data analysis and preparation of figures and tables was performed by L.P. supported by H.S. and G.K. Funding acquisition was done by G.K., D.H., and C.D. After draft writing by L.P. E.R. and G.K., all authors revised the manuscript. All authors have given approval to the final version of the manuscript.

Notes

The authors declare no competing financial interest.
The raw data can be downloaded free of charge using the following link: ftp://massive.ucsd.edu/v07/MSV000094712/

ACKNOWLEDGMENT

Parts of this project were funded by the City of Vienna Fund for Innovative Cancer Research (Project 21025) and the Austrian Science Fund (FWF, Project I6482-B, and Project KLI 1089). The authors thank all Koellensperger- and Rampler Lab members for their continuous support. Moreover, we want to express our gratitude for fruitful scientific discussions to Yasin El Abiead, Vinicius Verri Hernandes, Jean-Baptiste Vincendent, Rebekah Sayers, Andre Schreiber, Antonio Serna, David Cox, and Cagakan Ozbalci. We thank Hiroshi Tsugawa for his support with MS-DIAL.

REFERENCES

(1) Rampler, E.; Abiead, Y. El; Schoeny, H.; Rusz, M.; Hildebrand, F.; Fitz, V.; Koellensperger, G. Recurrent Topics in Mass Spectrometry-Based Metabolomics and Lipidomics - Standardization, Coverage, and Throughput. *Anal. Chem.* **2021**, *93* (1), 519–545. https://doi.org/10.1021/acs.analchem.0c04698.

(2) Cajka, T.; Fiehn, O. Toward Merging Untargeted and Targeted Methods in Mass Spectrometry-Based Metabolomics and Lipidomics. *Anal. Chem.* **2016**, *88* (1), 524–545. https://doi.org/10.1021/acs.analchem.5b04491.

(3) Koelmel, J. P.; Kroeger, N. M.; Gill, E. L.; Ulmer, C. Z.; Bowden, J. A.; Patterson, R. E.; Yost, R. A.; Garrett, T. J. Expanding Lipidome Coverage Using LC-MS/MS Data-Dependent Acquisition with Automated Exclusion List Generation. *J. Am. Soc. Mass Spectrom.* **2017**, *28* (5), 908–917. https://doi.org/10.1007/s13361-017-1608-0.

(4) Ivanisevic, J.; Want, E. J. From Samples to Insights into Metabolism: Uncovering Biologically Relevant Information in LC- HRMS Metabolomics Data. *Metabolites* **2019**, *9* (12), 1–30. https://doi.org/10.3390/metabo9120308.

(5) Defossez, E.; Bourquin, J.; von Reuss, S.; Rasmann, S.; Glauser, G. Eight Key Rules for Successful Data-Dependent Acquisition in Mass Spectrometry-Based Metabolomics. *Mass Spectrom. Rev.* **2023**, *42* (1), 131–143. https://doi.org/10.1002/mas.21715.

(6) Schwaiger, M.; Schoeny, H.; El Abiead, Y.; Hermann, G.; Rampler, E.; Koellensperger, G. Merging Metabolomics and Lipidomics into One Analytical Run. *Analyst* **2019**, *144* (1), 220–229. https://doi.org/10.1039/c8an01219a.

(7) Thompson, J. W.; Adams, K. J.; Adamski, J.; Asad, Y.; Borts, D.; Bowden, J. A.; Byram, G.; Dang, V.; Dunn, W. B.; Fernandez, F.; Fiehn, O.; Gaul, D. A.; Hühmer, A. F. R.; Kalli, A.; Koal, T.; Koeniger, S.; Mandal, R.; Meier, F.; Naser, F. J.; O'Neil, D.; Pal, A.; Patti, G. J.; Pham-Tuan, H.; Prehn, C.; Raynaud, F. I.; Shen, T.; Southam, A. D.; St. John-Williams, L.; Sulek, K.; Vasilopoulou, C. G.; Viant, M.; Winder, C. L.; Wishart, D.; Zhang, L.; Zheng, J.; Moseley, M. A. International Ring Trial of a High Resolution Targeted Metabolomics and Lipidomics Platform for Serum and Plasma Analysis. *Anal. Chem.* **2019**, *91*, 14407–14416. https://doi.org/10.1021/acs.analchem.9b02908.

(8) Bearden, D. W.; Sheen, D. A.; Simón-Manso, Y.; Benner, B. A.; Rocha, W. F. C.; Blonder, N.; Lippa, K. A.; Beger, R. D.; Schnackenberg, L. K.; Sun, J.; Mehta, K. Y.; Cheema, A. K.; Gu, H.; Marupaka, R.; Nagana Gowda, G. A.; Raftery, D. Metabolomics Test Materials for Quality Control: A Study of a Urine Materials Suite. *Metabolites* **2019**, *9* (11). https://doi.org/10.3390/metabo9110270.

(9) Lu, W.; McBride, M. J.; Lee, W. D.; Xing, X.; Xu, X.; Li, X.; Oschmann, A. M.; Shen, Y.; Bartman, C.; Rabinowitz, J. D. Selected Ion Monitoring for Orbitrap-Based Metabolomics. *Metabolites* **2024**, *14* (4), 184. https://doi.org/10.3390/metabo14040184.

(10) Amer, B.; Deshpande, R. R.; Bird, S. S. Simultaneous Quantitation and Discovery (SQUAD) Analysis: Combining the Best of Targeted and Untargeted Mass Spectrometry-Based Metabolomics. *Metabolites* **2023**, *13* (5), 648. https://doi.org/10.3390/metabo13050648.

(11) Melnik, A. V.; Da Silva, R. R.; Hyde, E. R.; Aksenov, A. A.; Vargas, F.; Bouslimani, A.; Protsyuk, I.; Jarmusch, A. K.; Tripathi, A.; Alexandrov, T.; Knight, R.; Dorrestein, P. C. Coupling Targeted and Untargeted Mass Spectrometry for Metabolome-Microbiome-Wide Association Studies of Human Fecal Samples. *Anal. Chem.* **2017**, *89* (14), 7549–7559. https://doi.org/10.1021/acs.analchem.7b01381.

(12) Rs Baker, P.; Proos, R. *Untargeted Data-Dependent Acquisition (DDA) Metabolomics Analysis Using the ZenoTOF 7600 System Source, Compound and Experimental Parameters to Perform DDA Experiments Using Collision-Induced Dissociation*; 2022. https://sciex.com/tech-notes/life-science-research/metabolomics/untargeted-data-dependent-acquisition--dda--metabolomics-analysis.

(13) Loboda, A. V.; Chernushevich, I. V. A Novel Ion Trap That Enables High Duty Cycle and Wide m/z Range on an Orthogonal Injection TOF Mass Spectrometer. *J. Am. Soc. Mass Spectrom.* **2009**, *20* (7), 1342–1348. https://doi.org/10.1016/j.jasms.2009.03.018.

(14) Sciex. *Qualitative Flexibility Combined with Quantitative Power*; 2021. https://sciex.com/tech-notes/technology/qualitative-flexibility-combined-with-quantitative-power---using.

(15) Huang, L.; Drouin, N.; Causon, J.; Wegrzyn, A.; Castro-Perez, J.; Fleming, R.; Harms, A.; Hankemeier, T. Reconstruction of Glutathione Metabolism in the Neuronal Model of Rotenone-Induced Neurodegeneration Using Mass Isotopologue Analysis with Hydrophilic Interaction Liquid Chromatography-Zeno High-Resolution Multiple Reaction Monitoring. *Anal. Chem.* **2022**. https://doi.org/10.1021/acs.analchem.2c04231.

(16) Ortmayr, K.; Schwaiger, M.; Hann, S.; Koellensperger, G. An Integrated Metabolomics Workflow for the Quantification of Sulfur Pathway Intermediates Employing Thiol Protection with N-Ethyl Maleimide and Hydrophilic Interaction Liquid Chromatography Tandem Mass Spectrometry. *Analyst* **2015**, *140* (22), 7687–7695. https://doi.org/10.1039/c5an01629k.

(17) Lv, W.; Wang, L.; Xuan, Q.; Zhao, X.; Liu, X.; Shi, X.; Xu, G. Pseudotargeted Method Based on Parallel Column Two-Dimensional Liquid Chromatography-Mass Spectrometry for Broad Coverage of Metabolome and Lipidome. *Anal. Chem.* **2020**, *92* (8), 6043–6050. https://doi.org/10.1021/acs.analchem.0c00372.

(18) Kim, S.; Jiang, W.; Chandler, J. D.; Fibrosis, C.; Medicine, S.; Ab, H. Analysis of Redox and Bioenergetics Metabolites with Polymeric IHILIC ® - (P) Classic HILIC Column and Mass Spectrometry. **2021**.

(19) El Abiead, Y.; Bueschl, C.; Panzenboeck, L.; Wang, M.; Doppler, M.; Seidl, B.; Zanghellini, J.; Dorrestein, P. C.; Koellensperger, G. Heterogeneous Multimeric Metabolite Ion Species Observed in LC-MS Based Metabolomics Data Sets. *Anal. Chim. Acta*

2022, *1229* (2022), 340352. https://doi.org/10.1016/j.aca.2022.340352.

(20) Tsugawa, H.; Ikeda, K.; Takahashi, M.; Satoh, A.; Mori, Y.; Uchino, H.; Okahashi, N.; Yamada, Y.; Tada, I.; Bonini, P.; Higashi, Y.; Okazaki, Y.; Zhou, Z.; Zhu, Z. J.; Koelmel, J.; Cajka, T.; Fiehn, O.; Saito, K.; Arita, M.; Arita, M. A Lipidome Atlas in MS-DIAL 4. *Nat. Biotechnol.* **2020**, *38* (10), 1159–1163. https://doi.org/10.1038/s41587-020-0531-2.

(21) Nothias, L. F.; Petras, D.; Schmid, R.; Dührkop, K.; Rainer, J.; Sarvepalli, A.; Protsyuk, I.; Ernst, M.; Tsugawa, H.; Fleischauer, M.; Aicheler, F.; Aksenov, A. A.; Alka, O.; Allard, P. M.; Barsch, A.; Cachet, X.; Caraballo-Rodriguez, A. M.; Da Silva, R. R.; Dang, T.; Garg, N.; Gauglitz, J. M.; Gurevich, A.; Isaac, G.; Jarmusch, A. K.; Kameník, Z.; Kang, K. Bin; Kessler, N.; Koester, I.; Korf, A.; Le Gouellec, A.; Ludwig, M.; Martin H, C.; McCall, L. I.; McSayles, J.; Meyer, S. W.; Mohimani, H.; Morsy, M.; Moyne, O.; Neumann, S.; Neuweger, H.; Nguyen, N. H.; Nothias-Esposito, M.; Paolini, J.; Phelan, V. V.; Pluskal, T.; Quinn, R. A.; Rogers, S.; Shrestha, B.; Tripathi, A.; van der Hooft, J. J. J.; Vargas, F.; Weldon, K. C.; Witting, M.; Yang, H.; Zhang, Z.; Zubeil, F.; Kohlbacher, O.; Böcker, S.; Alexandrov, T.; Bandeira, N.; Wang, M.; Dorrestein, P. C. Feature-Based Molecular Networking in the GNPS Analysis Environment. *Nat. Methods* **2020**, *17* (9), 905–908. https://doi.org/10.1038/s41592-020-0933-6.

(22) Wang, M.; Carver, J. J.; Phelan, V. V.; Sanchez, L. M.; Garg, N.; Peng, Y.; Nguyen, D. D.; Watrous, J.; Kapono, C. A.; Luzzatto-Knaan, T.; Porto, C.; Bouslimani, A.; Melnik, A. V.; Meehan, M. J.; Liu, W. T.; Crüsemann, M.; Boudreau, P. D.; Esquenazi, E.; Sandoval-Calderón, M.; Kersten, R. D.; Pace, L. A.; Quinn, R. A.; Duncan, K. R.; Hsu, C. C.; Floros, D. J.; Gavilan, R. G.; Kleigrewe, K.; Northen, T.; Dutton, R. J.; Parrot, D.; Carlson, E. E.; Aigle, B.; Michelsen, C. F.; Jelsbak, L.; Sohlenkamp, C.; Pevzner, P.; Edlund, A.; McLean, J.; Piel, J.; Murphy, B. T.; Gerwick, L.; Liaw, C. C.; Yang, Y. L.; Humpf, H. U.; Maansson, M.; Keyzers, R. A.; Sims, A. C.; Johnson, A. R.; Sidebottom, A. M.; Sedio, B. E.; Klitgaard, A.; Larson, C. B.; Boya, C. A. P.; Torres-Mendoza, D.; Gonzalez, D. J.; Silva, D. B.; Marques, L. M.; Demarque, D. P.; Pociute, E.; O'Neill, E. C.; Briand, E.; Helfrich, E. J. N.; Granatosky, E. A.; Glukhov, E.; Ryffel, F.; Houson, H.; Mohimani, H.; Kharbush, J. J.; Zeng, Y.; Vorholt, J. A.; Kurita, K. L.; Charusanti, P.; McPhail, K. L.; Nielsen, K. F.; Vuong, L.; Elfeki, M.; Traxler, M. F.; Engene, N.; Koyama, N.; Vining, O. B.; Baric, R.; Silva, R. R.; Mascuch, S. J.; Tomasi, S.; Jenkins, S.; Macherla, V.; Hoffman, T.; Agarwal, V.; Williams, P. G.; Dai, J.; Neupane, R.; Gurr, J.; Rodríguez, A. M. C.; Lamsa, A.; Zhang, C.; Dorrestein, K.; Duggan, B. M.; Almaliti, J.; Allard, P. M.; Phapale, P.; Nothias, L. F.; Alexandrov, T.; Litaudon, M.; Wolfender, J. L.; Kyle, J. E.; Metz, T. O.; Peryea, T.; Nguyen, D. T.; VanLeer, D.; Shinn, P.; Jadhav, A.; Müller, R.; Waters, K. M.; Shi, W.; Liu, X.; Zhang, L.; Knight, R.; Jensen, P. R.; Palsson, B.; Pogliano, K.; Linington, R. G.; Gutiérrez, M.; Lopes, N. P.; Gerwick, W. H.; Moore, B. S.; Dorrestein, P. C.; Bandeira, N. Sharing and Community Curation of Mass Spectrometry Data with Global Natural Products Social Molecular Networking. *Nat. Biotechnol.* **2016**, *34* (8), 828–837. https://doi.org/10.1038/nbt.3597.

(23) Pang, Z.; Chong, J.; Zhou, G.; De Lima Morais, D. A.; Chang, L.; Barrette, M.; Gauthier, C.; Jacques, P. É.; Li, S.; Xia, J. MetaboAnalyst 5.0: Narrowing the Gap between Raw Spectra and Functional Insights. *Nucleic Acids Res.* **2021**, *49* (W1), W388–W396. https://doi.org/10.1093/nar/gkab382.

(24) Pang, Z.; Zhou, G.; Ewald, J.; Chang, L.; Hacariz, O.; Basu, N.; Xia, J. Using MetaboAnalyst 5.0 for LC–HRMS Spectra Processing, Multi-Omics Integration and Covariate Adjustment of Global Metabolomics Data. *Nat. Protoc.* **2022**, *17* (8), 1735–1761. https://doi.org/10.1038/s41596-022-00710-w.

(25) Torp, S. H.; Solheim, O.; Skjulsvik, A. J. The WHO 2021 Classification of Central Nervous System Tumours: A Practical Update on What Neurosurgeons Need to Know—a Minireview. *Acta Neurochir. (Wien).* **2022**, *164* (9), 2453–2464. https://doi.org/10.1007/s00701-022-05301-y.

(26) Wishart, D. S.; Guo, A. C.; Oler, E.; Wang, F.; Anjum, A.; Peters, H.; Dizon, R.; Sayeeda, Z.; Tian, S.; Lee, B. L.; Berjanskii, M.; Mah, R.; Yamamoto, M.; Jovel, J.; Torres-Calzada, C.; Hiebert-Giesbrecht, M.; Lui, V. W.; Varshavi, D.; Varshavi, D.; Allen, D.; Arndt, D.; Khetarpal, N.; Sivakumaran, A.; Harford, K.; Sanford, S.; Yee, K.; Cao, X.; Budinski, Z.; Liigand, J.; Zhang, L.; Zheng, J.; Mandal, R.; Karu, N.; Dambrova, M.; Schiöth, H. B.; Greiner, R.; Gautam, V. HMDB 5.0: The Human Metabolome Database for 2022. *Nucleic Acids Res.* **2022**, *50* (D1), D622–D631. https://doi.org/10.1093/nar/gkab1062.

(27) Fenaille, F.; Barbier Saint-Hilaire, P.; Rousseau, K.; Junot, C. Data Acquisition Workflows in Liquid Chromatography Coupled to High Resolution Mass Spectrometry-Based Metabolomics: Where Do We Stand? *J. Chromatogr. A* **2017**, *1526*, 1–12. https://doi.org/10.1016/j.chroma.2017.10.043.

(28) Phinney, K. W.; Ballihaut, G.; Bedner, M.; Benford, B. S.; Camara, J. E.; Christopher, S. J.; Davis, W. C.; Dodder, N. G.; Eppe, G.; Lang, B. E.; Long, S. E.; Lowenthal, M. S.; McGaw, E. A.; Murphy, K. E.; Nelson, B. C.; Prendergast, J. L.; Reiner, J. L.; Rimmer, C. A.; Sander, L. C.; Schantz, M. M.; Sharpless, K. E.; Sniegoski, L. T.; Tai, S. S. C.; Thomas, J. B.; Vetter, T. W.; Welch, M. J.; Wise, S. A.; Wood, L. J.; Guthrie, W. F.; Hagwood, C. R.; Leigh, S. D.; Yen, J. H.; Zhang, N. F.; Chaudhary-Webb, M.; Chen, H.; Fazili, Z.; Lavoie, D. J.; McCoy, L. F.; Momin, S. S.; Paladugula, N.; Pendergrast, E. C.; Pfeiffer, C. M.; Powers, C. D.; Rabinowitz, D.; Rybak, M. E.; Schleicher, R. L.; Toombs, B. M. H.; Xu, M.; Zhang, M.; Castle, A. L. Development of a Standard Reference Material for Metabolomics Research. *Anal. Chem.* **2013**, *85* (24), 11732–11738. https://doi.org/10.1021/ac402689t.

(29) Schoeny, H.; Rampler, E.; El Abiead, Y.; Hildebrand, F.; Zach, O.; Hermann, G.; Koellensperger, G. A Combined Flow Injection/Reversed-Phase Chromatography-High-Resolution Mass Spectrometry Workflow for Accurate Absolute Lipid Quantification with 13C Internal Standards. *Analyst* **2021**, *146* (8), 2591–2599. https://doi.org/10.1039/d0an02443k.

(30) El Abiead, Y.; Milford, M.; Salek, R. M.; Koellensperger, G. MzRAPP - A Tool for Reliability Assessment of Data Pre-Processing in Non-Targeted Metabolomics. *Bioinformatics* **2021**, 2–4. https://doi.org/10.1093/bioinformatics/btab231.

(31) Safari Yazd, H.; Bazargani, S. F.; Fitzpatrick, G.; Yost, R. A.; Kresak, J.; Garrett, T. J. Metabolomic and Lipidomic Characterization of Meningioma Grades Using LC-HRMS and Machine Learning. *J. Am. Soc. Mass Spectrom.* **2023**, *34* (10), 2187–2198. https://doi.org/10.1021/jasms.3c00158.

(32) Bender, L.; Somme, F.; Ruhland, E.; Cicek, A. E.; Bund, C.; Namer, I. J. Metabolomic Profile of Aggressive Meningiomas by Using High-Resolution Magic Angle Spinning Nuclear Magnetic Resonance. *J. Proteome Res.* **2020**, *19* (1), 292–299. https://doi.org/10.1021/acs.jproteome.9b00521.

(33) Masalha, W.; Daka, K.; Woerner, J.; Pompe, N.; Weber, S.; Delev, D.; Krüger, M. T.; Schnell, O.; Beck, J.; Heiland, D. H.; Grauvogel, J. Metabolic Alterations in Meningioma Reflect the Clinical Course. *BMC Cancer* **2021**, *21* (1), 1–9. https://doi.org/10.1186/s12885-021-07887-5.

(34) Corey, M. G.; Joshua, L.; John, W. R.; Hanane, A.; Nancy, F.; Ying-Chih, W.; Nataly, F.; Margaret, P.; Melissa, U.; Yayoi, K.; Russell, B. M. B.; Joshua, B.; Michael, D.; Melissa, S.; Robert, S.; Raj, K. S.; Mary, F. Recurrent IDH Mutations in High-Grade Meningioma. *Neuro. Oncol.* **2020**, *22* (7), 1044–1045. https://doi.org/10.1093/neuonc/noaa065.

(35) Broeckling, C. D.; Beger, R. D.; Cheng, L. L.; Cumeras, R.; Cuthbertson, D. J.; Dasari, S.; Davis, W. C.; Dunn, W. B.; Evans, A. M.; Fernández-Ochoa, A.; Gika, H.; Goodacre, R.; Goodman, K. D.; Gouveia, G. J.; Hsu, P. C.; Kirwan, J. A.; Kodra, D.; Kuligowski, J.; Lan, R. S. L.; Monge, M. E.; Moussa, L. W.; Nair, S. G.; Reisdorph, N.; Sherrod, S. D.; Ulmer Holland, C.; Vuckovic, D.; Yu, L. R.; Zhang, B.; Theodoridis, G.; Mosley, J. D. Current Practices in LC-MS Untargeted Metabolomics: A Scoping Review on the Use of Pooled Quality Control Samples. *Anal. Chem.* **2023**, *95* (51), 18645–18654. https://doi.org/10.1021/acs.analchem.3c02924.

(36) Vermeulen, C.; Pagès-Gallego, M.; Kester, L.; Kranendonk, M. E. G.; Wesseling, P.; Verburg, N.; de Witt Hamer, P.; Kooi, E. J.; Dankmeijer, L.; van der Lugt, J.; van Baarsen, K.; Hoving, E. W.; Tops, B. B. J.; de Ridder, J. Ultra-Fast Deep-Learned CNS Tumour Classification during Surgery. *Nature* **2023**, *622* (7984), 842–849. https://doi.org/10.1038/s41586-023-06615-2.

Insert Table of Contents artwork here